Microscopic origin of the π states in epitaxial silicene

A. Fleurence,[1,a)] Y. Yoshida,[2] C.-C. Lee,[1] T. Ozaki,[1,3] Y. Yamada-Takamura,[1] and Y. Hasegawa[2]

[1]*School of Materials Science, Japan Advanced Institute of Science and Technology, 1-1 Asahidai, Ishikawa 923-1292, Japan*

[2]*The Institute for Solid State Physics, The University of Tokyo, Kashiwanoha 5-1-5, Kashiwa, Chiba 277-8581, Japan*

[3]*Research Center for Simulation Science, Japan Advanced Institute of Science and Technology, 1-1 Asahidai, Ishikawa 923-1292, Japan*

(Received 4 October 2013; accepted 28 December 2013; published online 16 January 2014)

We investigated the electronic properties of epitaxial silicene on $ZrB_2(0001)$ thin film grown on Si(111) by means of low-temperature scanning tunneling spectroscopy and density functional theory calculations. The position of silicon atoms and thus, the localization of the valence and conduction states were deducted from the comparison of the spectra and the computed local density of states. We point out the strong contribution of p_z orbitals of specific atoms to those states which indicates the π character of the conduction and valence bands. A clear correlation between hybridization of the orbitals of the Si atoms and the buckling was evidenced. © *2014 AIP Publishing LLC*. [http://dx.doi.org/10.1063/1.4862261]

Silicene, the graphene-like allotrope of silicon is the object of a recently raised enthusiasm, due to the perspectives opened by the novelty of its electronic, physical, and chemical properties. Those derive from the electronic band structure of this atom thick honeycomb structure made of silicon atoms characterized by a π electronic system, which, in the hypothetical free-standing form of silicene, gives rise to Dirac cones.[1,2] Nevertheless, owing to a stronger spin-orbit coupling, the quantum spin Hall effect is predicted to be observable and switchable by a vertical electric field[3,4] leading to the suggestion of spin-polarized electron source devices based on silicene.[5] This appealing property derives from the crystal structure of silicene, which differs from that of planar graphene by the buckling of the honeycomb structure and the intermediate sp^2/sp^3 hybridization of the orbitals of the Si atoms required to sustain the cohesion of silicene in spite of the larger distance between nearest-neighbors.[1] Silicene, however, only exists in epitaxial forms, that differ from the free-standing one by their reconstructed structures and their less trivial bucklings. Si honeycomb structures can be grown by deposition of silicon atoms on substrates such as Ag(110),[6,7] Ag(111),[8–16] or Ir(111).[17] Whereas for the latter system no characterization of the electronic properties has been reported, silicene nanoribbons[7,18] and two-dimensional sheets on Ag[13,16] show signatures of π bands.

Silicene alternatively forms in a spontaneous and self-terminating way by the crystallization of Si atoms segregating on the (0001) surface of zirconium diboride (ZrB_2) thin films grown on Si(111)[19] giving rise to a homogenous two-dimensional silicene sheet covering the whole surface. Although the epitaxial relationship induces a $(\sqrt{3} \times \sqrt{3})$-reconstruction of silicene due to the registry of this unit cell with the (2×2) unit cell of $ZrB_2(0001)$, the observation of intact $ZrB_2(0001)$ surface states indicates a minor degree of coupling of silicene with the Zr-terminated surface.[19–21] The band structure differs from that of free-standing silicene by the opening of a gap which was found to be a direct consequence of the specific buckling resulting from the $(\sqrt{3} \times \sqrt{3})$ reconstruction.[19,22] This demonstrates that silicene has the merit compared to its carbon analogue graphene to have its electronic band structure transformable owing to the flexibility of its internal structure which is allowed by a tunable mixed sp^2/sp^3 hybridization of the silicon atoms.

To understand how the deviation of the buckling from that of free-standing silicene affects the electronic properties, we carried out a mapping of the local density of states (LDOS) giving insight on the microscopic origin of the electronic states of silicene. The comparison of the experimental results with density functional theory (DFT) calculations has shown a consistent correspondence, from which the position of the reconstructed $(\sqrt{3} \times \sqrt{3})$ unit cell with respect to the scanning tunneling microscope (STM) image can be deduced and the contribution of each individual silicon atom can be evaluated.

Samples were prepared following a method described elsewhere.[19,20] STM and scanning tunneling spectroscopy (STS) experiments were carried out in a dedicated low-noise low-temperature setup cooled down to 5.5 K and using an electrochemically etched W tip. The mapping of the LDOS consists of 64×64 tunneling conductance dI/dV spectra recorded in a $2\,\text{nm} \times 2\,\text{nm}$ square. The dI/dV images are formed by collecting the conductance values measured at specific sample bias voltages. Before taking each spectrum, the tip-surface distance is adjusted by closing the feed-back loop and setting the current set point and V the sample bias voltage to 0.5 nA and 0.5 V, respectively. The tunneling conductance dI/dV spectra were recorded by means of a lock-in detection method using a 9.284 kHz-modulated sample bias voltage with an amplitude of $40\,\text{mV}_{rms}$. DFT calculations within a generalized gradient approximation[23,24] have been performed using the OpenMX code, which is based on norm-conserving pseudopotentials generated with multireference energies[25] and optimized pseudoatomic basis

a)Author to whom correspondence should be addressed. Electronic mail: antoine@jaist.ac.jp

functions.[26] Further computational details can be found elsewhere.[22] The optimized silicene structure is presented in Fig. 1(a). Among the six Si atoms of the $(\sqrt{3}\times\sqrt{3})$ unit cell, two are sitting on hollow sites of the Zr-terminated ZrB_2 surface (called A atoms, hereafter), three, at positions between a bridge site and a Zr atom (B atoms), and one is sitting on top of a Zr atom (C atom).[19,22] Although metastable in the calculations,[22] this structure has shown good agreement with experimental results[19] including those unveiled in the present paper, and is thus relevant to give insight into the origin of the spectral features observed experimentally. The buckling of the structure deviates from that predicted for free-standing silicene by the position of the C atom, which is lifted up to almost the height of the B atoms. It is due to the fact that the A and C atoms, which belong to the same sub-lattice, are sitting on the most and least favorable positions on $ZrB_2(0001)$, respectively.[22] The Si-Si bond lengths are approximately 2.25 Å, in agreement with calculations for free-standing-silicene[1] and with other epitaxial silicene systems,[12,18] and are significantly shorter than that of bulk silicon where atoms are sp^3-hybridized.

Although by using a particularly sharp tip, the silicene honeycomb structure can be resolved,[19] more often the surface appears on constant-current STM image as a $(\sqrt{3}\times\sqrt{3})$ array of protrusions similar to that shown in Fig. 1(b), where the orientation of the silicene honeycomb structure cannot be assigned without disambiguation. This low-temperature image resembles those recorded at room temperature[19,20] and does not reveal any structural phase transition as for the $(\sqrt{3}\times\sqrt{3})$-reconstructed form of silicene on Ag(111).[14] The spectra recorded at positions (1) to (9) as assigned in Fig. 1(b) are plotted in Fig. 2. For all spectra, an approximately 350 meV-wide gap whose center is shifted by 60 meV below the Fermi level ($V=0$ V), is observed. In spite of a non-zero value of the tunneling conductance in the gap due to the metallic nature of ZrB_2, those data confirm the semiconducting character of epitaxial silicene on ZrB_2 evidenced by angle-resolved ultraviolet photoemisssion

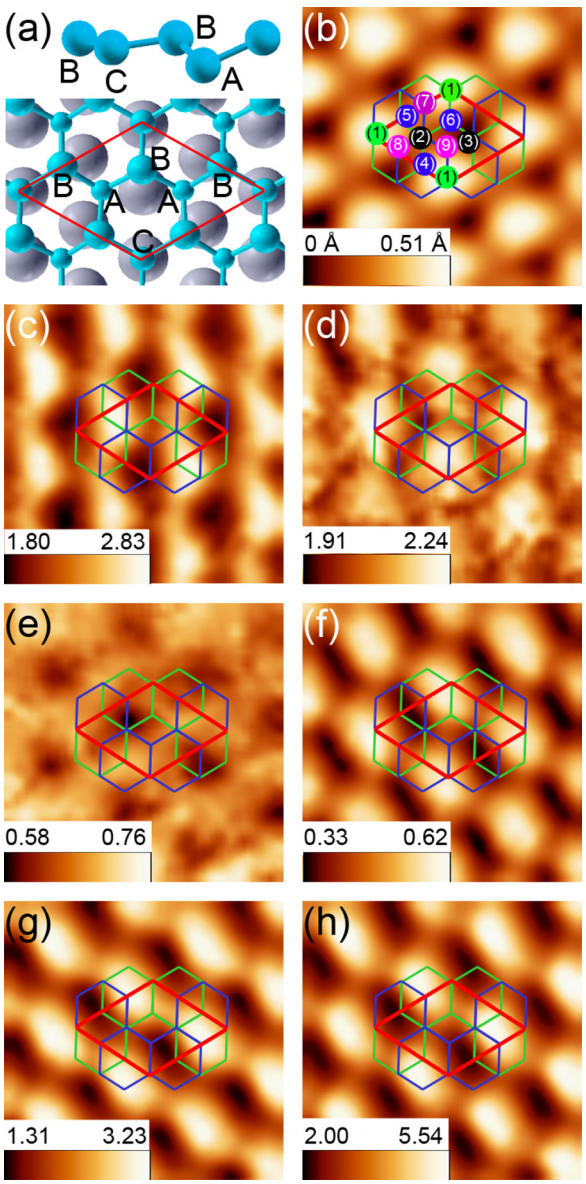

FIG. 1. Mapping of the LDOS of epitaxial silicene on $ZrB_2(0001)$. (a) Structure of epitaxial silicene on $ZrB_2(0001)$ derived from DFT calculations. The height of the Si atoms (colored in blue) with respect to the Zr atoms (colored in grey) of the uppermost layer are 2.124 Å, 3.062 Å, and 2.727 Å for the A, B, and C atoms, respectively. (b) STM image (2 nm × 2 nm, $V=-0.50$ V, and $I=500$ pA) recorded in the current-constant mode. (c) to (h) dI/dV tunneling conductance images at the sample bias voltages of the features denoted (*i*) to (*vi*) as identified in the spectra displayed in Fig. 2: $V=-0.47$ V, $V=-0.36$ V, $V=-0.12$ V, $V=-0.02$ V, $V=0.20$ V, and $V=0.36$ V. The red rhombus emphasizes the $(\sqrt{3}\times\sqrt{3})$ unit cell. The two possible orientations of the honeycomb structure are shown in different colors. The amplitude of the color-coded scale is indicated.

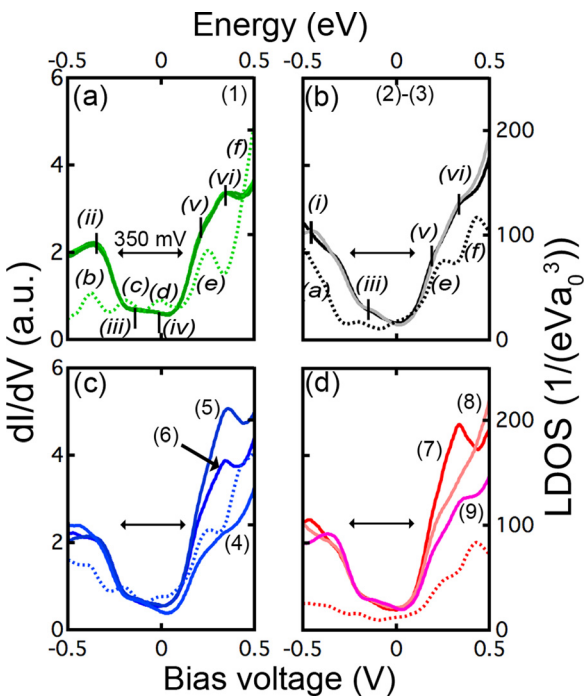

FIG. 2. The local electronic structure of epitaxial silicene on $ZrB_2(0001)$. Solid curves represent the dI/dV tunneling conductance spectra recorded at (a) positions (1) as indicated in Fig. 1(b), (b) positions (2) and (3), (c) positions (4), (5), and (6), and (d) positions (7), (8), and (9) plotted as functions of the sample bias voltage. Dashed curves represent the computed LDOS above (a) C atom, (b) the A atom, (c) the B atom, and (d) the center of the hexagons of the honeycomb lattice plotted as functions of the energy. a_0 is the Bohr radius. The distance to silicene as defined by the average height of the Si atoms are, respectively, 6.0 Å, 5.6 Å, 5.8 Å, and 5.8 Å. Spectral features in the tunneling conductance and in the calculated LDOS are denoted (*i*) to (*vi*) and (*a*) to (*f*), respectively.

spectroscopy (ARUPS).[19] In addition, several features corresponding to images Figs. 1(c) to 1(h) were identified. For the filled states, two features, labelled (*i*) and (*ii*), are observed. The former is in the vicinity of the lower limit of the bias voltage range, and the latter, centered on $V = -0.36$ V, extends up to the gap edge at -0.23 V. Thus, it coincides with the maxima of the parabolic valence band observed at the K_{Si}, the K point of the Brillouin zone of the unreconstructed silicene.[19,21] Whereas feature (*i*) is located around positions (2), (3), and (5), feature (*ii*) appears centered on position (1) with some extension to the positions (4), (5), and (6) (Fig. 1(c)). Within the gap, two low-intensity features labelled (*iii*) and (*iv*) are identified. The first one, around $V = -0.12$ V, has a weak spatial dependence and is observed for all positions. It can therefore be attributed to the metallic $ZrB_2(0001)$ surface states. On the contrary, the second one at (*iv*) $V = -0.02$ V has a similar spatial dependence to that of feature (*ii*). In the empty states, two features labelled (*v*) and (*vi*) both centered on position (7) and extending to neighboring positions (see Figs. 1(g) and 1(h)) are observed around $V = 0.20$ V and $V = 0.36$ V. The first one which extends down to the energy gap at 0.10 V above the Fermi level can be associated to the conduction band predicted to exist in the middle between Γ and K_{Si} points.[22] This band was experimentally observed by ARUPS, owing to a significant electron donation from K adatoms which shifts it below the Fermi level.[21]

To establish a connection between the different features listed above and the atomic and electronic structure of silicene, the LDOS has been calculated by the integration of the electronic states in the interval of 20 meV at each point of the real-space grid. The LDOS at selected positions above the silicene sheet are shown in Fig. 2. The distance to the surface is adjusted to be consistent with the profile of the STM image of Fig. 1(b). The relevance of the silicene structure of Fig. 1(a) for the comparison with experimental results is verified by the width and the position of the computed energy gap. Moreover, several features in the computed LDOS have their counterparts in the experimental results. Indeed, features labelled (*a*) to (*f*) centered on $V = -0.45$ V, $V = -0.38$ V, $V = -0.19$ V, $V = -0.02$ V, $V = 0.27$ V, and $V = 0.45$ V can be assigned to the spectral features (*i*) to (*vi*). Similarities between the spatial dependences of the tunneling conductance and the computed LDOS can also be found. The resemblance of the calculated LDOS above the C atom with spectra recorded at position (1), emphasized by the consistent absence of features (*i*) and (*a*), indicates that the protrusions observed on the STM image of Fig. 1(a) coincide with these atoms. The assignment of positions (1) to the C atom is consistent with its singular place within the $(\sqrt{3} \times \sqrt{3})$ unit cell and the uppermost position of this atom together with its nearest-neighbors, the B atoms. The comparison of the LDOS calculated for the A atoms and the dI/dV curves recorded at positions (2) and (3) further confirm the above statement (Fig. 2(b)). Indeed, the strength of feature (*a*) and the weakness of feature (*b*) together with the respective intensities of features (*e*) and (*f*) are all together in agreement with the shape of the dI/dV curves recorded at positions (2) and (3). Finally, the comparison of the dI/dV curves and the LDOSs plotted in Figs. 2(c) and 2(d) suggests that positions (4), (5), and (6) are therefore corresponding to the sites of B atoms rather than to positions (7), (8), and (9), which therefore are attributed to the center of the hexagons of the honeycomb lattice. The silicene structure thus coincides with the green-colored honeycomb lattice shown in Fig. 1.

While the density of states per real-space grid (LDOS) can be compared with the STS data, the density of states (DOS) per atomic orbital is also informative since it provides indications on the atomic origin of the spectral features. In particular, the weight of the respective contributions of the s, p_x, p_y, and p_z orbitals to the electronic states can tell us the degree of hybridization of the orbitals for each considered Si atom. The intermediate hybridization of a system between sp^2 and sp^3 indicates how much the p_z orbital merges with the s, p_x, and p_y orbitals, which in a purely sp^2-hybridized system form three equivalent σ bonds with the nearest neighbors, whereas the bonding between p_z orbitals give rise to π states. The out-of-plane p_z orbital has therefore to be distinguished from the in-plane s, p_x, and p_y orbitals (the sp^2 orbitals). For a given eigen energy, the hybridization of the orbitals can be expressed by sp^{2+x}, where $x = 3DOS(p_z)/DOS(sp^2)$ for $DOS(sp^2) > 3DOS(p_z)$ and $x = DOS(sp^2)/3DOS(p_z)$ for $DOS(sp^2) < 3DOS(p_z)$.[27] $DOS(s)$, $DOS(p_x)$, $DOS(p_y)$, and $DOS(p_z)$ are the respective DOS of the s, p_x, p_y, and p_z orbitals and $DOS(sp^2) = DOS(s) + DOS(p_x) + DOS(p_y)$.

For each different Si atom in the $(\sqrt{3} \times \sqrt{3})$-reconstruction, $DOS(p_z)$, $DOS(sp^2)$, and x are plotted in Fig. 3 as functions of the eigen energy. One can observe that the features labelled (*b*), (*e*), and (*f*) in Fig. 2 reproducing the valence and conduction states (*ii*), (*v*), and (*vi*), correspond to an intense peak in the $DOS(p_z)$ of the C atom. The hybridization for this atom is approximately $sp^{2.1}$. The B and A atoms contribute to a less extent to those features. Whereas for the valence states the hybridization for both atoms is approximately $sp^{2.3}$ with a dominant contribution of the p_z orbitals, the contributions to

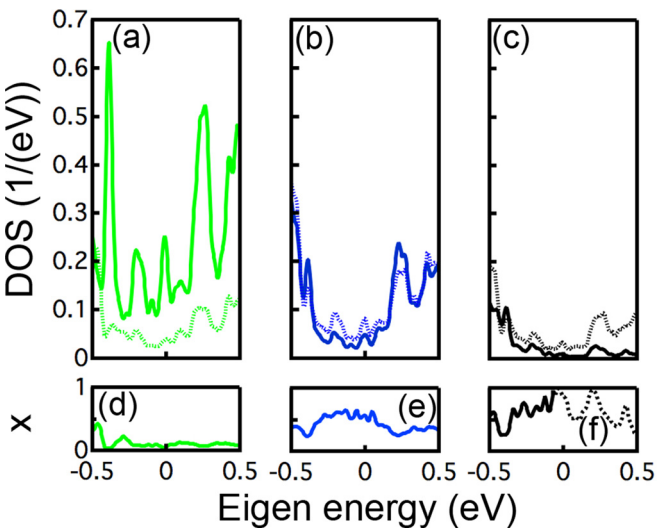

FIG. 3. Contribution to the eigen states of the orbitals of the Si atoms in epitaxial silicene. (a)–(c): DOS of the p_z ($DOS(p_z)$, thick line) and sum of the DOS of the s, p_x, and p_y orbitals ($DOS(sp^2)$, thin line) for the C, B, and A silicon atoms, respectively. For the latter two, a single atom of the $(\sqrt{3} \times \sqrt{3})$ reconstruction is considered. (d)–(f): x for the C, B, and A atoms, respectively. Solid and dashed lines represent, respectively, the rather p_z ($3DOS(p_z) > DOS(sp^2)$) and sp^2-character ($3DOS(p_z) < DOS(sp^2)$) of the contribution.

the conduction states differ from each other. The B atoms have a contribution similar to that for the valence states and for the A atoms, the contribution is in average closer to that of a sp^3-hybridized atom. The weight of the p_z orbitals of the Si atoms indicates the π character of the valence and conduction bands observed by ARUPS. The contribution of the p_z orbitals of the C atom to the conduction and valence states (*ii*), (*v*), and (*vi*) is consistent with the position of those features (see Fig. 1) and the position of this specific atom as determined previously. The shift of the features observed on Figs. 1(g) and 1(h) towards position (7) suggests the breaking of the rotational symmetry in the silicene structure in relation with the texturation into ribbon-shaped stress domains.[19] As the domain superstructure was not taken into account in the calculation, the possible slight difference between the B atoms cannot be reflected.

The so-evaluated hybridization of the orbitals of the different Si atoms is, however, in agreement with the internal structure of epitaxial silicene as shown on Fig. 1(a). The C atom has a coordination very close to that of a purely sp^2-hybridized atom since the angle between its nearest-neighbors is 117°, whereas it is 104.1° for A atom, 104.9° and 115.2° for B atoms.[19] One can deduce that the epitaxial relationship with the $ZrB_2(0001)$ surface shifts the hybridization of the orbitals of the A and C atoms, which belong to the same sub-lattice, respectively, towards sp^3 for the former and towards sp^2 for the latter. As a consequence of the breaking of the translational symmetry, the π-system of silicene, which features Dirac cones in the hypothetical free-standing form, is transformed into parabolic conduction and valence bands separated by a gap.

In conclusion, by means of low-temperature STM and STS, we measured the band gap and demonstrate the n-type semiconducting nature of epitaxial silicene on $ZrB_2(0001)$. With a strong support from DFT calculations, the mapping of the LDOS allows the determination of the position of the Si atoms of epitaxial silicene and the assignment of the different spectral features to specific silicon orbitals. In particular, the previously resolved bands π and π^* were attributed to originate predominantly from the p_z orbitals of the Si atoms sitting on top of Zr atoms, whose conformation is close to that of carbon atoms in graphene.

We are grateful to Professor Rainer Friedlein for fruitful discussion and the critical reading of the manuscript. This work was supported by KAKENHI (No. 24810011), NEXT program (GR046), and also by the joint research program of the Institute for Solid State Physics, the University of Tokyo.

[1]S. Cahangirov, M. Topsakal, E. Aktürk, H. Şahin, and S. Ciraci, Phys. Rev. Lett. **102**, 236804 (2009).
[2]C.-C. Liu, W. Feng, and Y. Yao, Phys. Rev. Lett. **107**, 076802 (2011).
[3]M. Ezawa, New J. Phys. **14**, 033003 (2012).
[4]M. Ezawa, Phys. Rev. Lett. **110**, 026603 (2013).
[5]W.-F. Tsai, C.-Y. Huang, T.-R. Chang, H. Lin, H.-T. Jeng, and A. Bensil, Nat. Commun. **4**, 1500 (2013).
[6]P. De Padova, P. Perfetti, B. Olivieri, C. Quaresima, C. Ottaviani, and G. Le Lay, J. Phys.: Condens. Matter **24**, 223001 (2012).
[7]P. De Padova, O. Kubo, B. Olivieri, C. Quaresima, T. Nakayama, M. Aono, and G. Le Lay, Nano Lett. **12**, 5500 (2012).
[8]C.-L. Lin, R. Arafune, K. Kawahara, N. Tsukahara, E. Minamitani, Y. Kim, N. Takagi, and M. Kawai, Appl. Phys. Express **5**, 045802 (2012).
[9]B. Feng, Z. Ding, S. Meng, Y. Yao, X. He, P. Cheng, L. Chen, and K. Wu, Nano Lett. **12**, 3507 (2012).
[10]H. Jamgotchian, Y. Colignon, N. Hamzaoui, B. Ealet, J. Y. Hoarau, B. Aufray, and J. P. Bibérian, J. Phys.: Condens. Matter **24**, 172001 (2012).
[11]D. Chiappe, C. Grazianetti, G. Tallarida, M. Fanciulli, and A. Molle, Adv. Mater. **24**, 5088 (2012).
[12]P. Vogt, P. De Padova, C. Quaresima, J. Avila, E. Frantzeskakis, M. C. Asensio, A. Resta, B. Ealet, and G. Le Lay, Phys. Rev. Lett. **108**, 155501 (2012).
[13]L. Chen, C.-C. Liu, B. Feng, X. He, P. Cheng, Z. Ding, S. Meng, Y. Yao, and K. Wu, Phys. Rev. Lett. **109**, 056804 (2012).
[14]L. Chen, H. Li, B. Feng, Z. Ding, J. Qiu, P. Cheng, K. Wu, and S. Meng, Phys. Rev. Lett. **110**, 085504 (2013).
[15]L. Chen, B. Feng, and K. Wu, Appl. Phys. Lett. **102**, 081602 (2013).
[16]P. De Padova, P. Vogt, A. Resta, J. Avila, I. Razado-Colambo, C. Quaresima, C. Ottaviani, B. Olivieri, T. Bruhn, T. Hirahara *et al.*, Appl. Phys. Lett. **102**, 163106 (2013).
[17]L. Meng, Y. Wang, L. Zhang, S. Du, R. Wu, L. Li, Y. Zhang, G. Li, H. Zhou, W. A. Hofer *et al.*, Nano Lett. **13**, 685 (2013).
[18]P. De Padova, C. Quaresima, C. Ottaviani, P. M. Sheverdyaeva, P. Moras, C. Carbone, D. Topwal, B. Olivieri, A. Kara, H. Oughaddou *et al.*, Appl. Phys. Lett. **96**, 261905 (2010).
[19]A. Fleurence, R. Friedlein, T. Ozaki, H. Kawai, Y. Wang, and Y. Yamada-Takamura, Phys. Rev. Lett. **108**, 245501 (2012).
[20]Y. Yamada-Takamura, F. Bussolotti, A. Fleurence, S. Bera, and R. Friedlein, Appl. Phys. Lett. **97**, 073109 (2010).
[21]R. Friedlein, A. Fleurence, J. T. Sadowski, and Y. Yamada-Takamura, Appl. Phys. Lett. **102**, 221603 (2013).
[22]C.-C. Lee, A. Fleurence, R. Friedlein, Y. Yamada-Takamura, and T. Ozaki, Phys. Rev. B **88**, 165404 (2013).
[23]J. P. Perdew, K. Burke, and M. Ernzerhof, Phys. Rev. Lett. **77**, 3865 (1996).
[24]W. Kohn and L. J. Sham, Phys. Rev. **140**, A1133 (1965).
[25]I. Morrison, D. Bylander, and L. Kleinman, Phys. Rev. B **47**, 6728 (1993).
[26]T. Ozaki, Phys. Rev. B **67**, 155108 (2003).
[27]See supplemental material at http://dx.doi.org/10.1063/1.4862261 for an explanation of the expressions used to calculate the hybridization.